VELOCITY-SPACE SYNTHESIS OF ISEE-1 MEASUREMENTS OF THE THREE-DIMENSIONAL ELECTRON DISTRIBUTION FUNCTION

by

R. J. Fitzenreiter
J. D. Scudder
NASA/Goddard Space Flight Center
Laboratory for Extraterrestrial Physics
Greenbelt, MD 20771

I. INTRODUCTION

This document describes a computer package which produces contour plots of the three-dimensional electron distribution function measured by the GSFC electron spectrometer aboard ISEE-1 (Ogilvie et al., 1978). The instrument configuration consists of three opposed pairs of analyzers whose alignments are mutually orthogonal. Thus, at any instant, the instrument is looking along both senses of each of the three orthogonal axes, as shown in Figure 1a. The timing and energy steps of the electron energy spectrum measurement is shown in Figure 1b. In one sweep through the 16 electron velocity steps of the instrument, the spacecraft rotates through one sector, or one-sixth of a complete revolution sampling phase space at 96 (16 x 6) points in 0.5 seconds. The electron velocity sweep repeats during each sector and one complete 3 second spin of the spacecraft observes at 576 (6 x 96) discrete points on the distribution function, $f(\vec{V}(t))$, which, as a surface, resides in a 4-space whose coordinates are $(V_x(t), V_y(t), V_z(t), f(V_x(t), V_x(t), V_z(t))$. The implicit relationship on time given by $\vec{V}(t)$ is due to the magnitude and direction of the sampled velocity vectors being determined by the energy sweep and the spin rate, respectively.

A model-independent graphical representation of the measured $f(\vec{V}(t))$ is illustrated in Figure 2 which shows 2-dimensional cuts of the full $f(\vec{V}(t))$ surface for one spin. The two dimensional trace is defined by

$$f(\vec{V} \cdot \hat{n}_i(t)) \text{ vs } \vec{V} \cdot \hat{n}_i(t) > 0, \text{ and}$$

$$f(\vec{V} \cdot \hat{n}_j(t)) \text{ vs } \vec{V} \cdot n_j(t) < 0$$

for opposed sensors which by hardware construction have anti-colinear fields of view, $\hat{n}_i \cdot \hat{n}_j = -1$. Data from opposed sensors have a common symbol. Thus each panel in Figure 2 displays data from three pairs of opposed sensors rotated into a common plane to facilitate comparison. The six panels show data from successive 0.5 second energy sweeps and 60° rotations of the spacecraft. Although each "slice" of the $f(\vec{V}(t))$ surface shown by these 2-dimensional traces allow model-independent determinations of anisotropies in the distribution function, a more complete picture of

the plasma microstate could be obtained if the four dimensional $f(\vec{V}(t))$ surface itself could be represented.

Except in high gradient regimes, the electron plasma is gyrotropic in the proper frame, i.e., the frame that is at rest relative to the bulk flow. This results in a cylindrical symmetry about the magnetic field direction which reduces the 4-space to three-dimensions ($W_{\parallel}(t)$, $W_{\perp}(t)$, $f(W_{\parallel}(t), W_{\perp}(t))$, thus collapsing the distribution to reside in a 3-space which can be contoured. The electron speeds $W_{\parallel}$ and $W_{\perp}$ are the proper frame parallel and perpendicular components of the observed velocities. This transformation has been used to assemble the 2-dimensional cuts of the distribution function in Figure 2 as the contour plot of Figure 3a. The coordinates are $W_{\perp}$ and $W_{\parallel}$ and the contours indicate levels where the distribution function is a constant. The separation of the contours correspond to variations in the natural logarithm of the distribution function equal to unity. The dotted lines show the "tracks" in $W_{\perp}$, $W_{\parallel}$ space along which the observations actually lie, and the gaps between observations are filled, in this space, with a two dimensional spline procedure. In Figure 3b, a gray shaded version of the contour plot of $f(W_{\parallel}(t), W_{\perp}(t))$ is shown. The level of gray shading is proportional to the logarithm of the distribution function and the white lines indicate discrete iso-contours.

Either of these plots are a product of this computer package at the option of the user. The line contours provide a higher resolution display than the gray shaded contours but require more computer time, approximately 45 seconds CPU/IO time for each line plot and approximately 10 seconds for each gray plot. The remainder of this report will document the use of the program: Section II contains a description of the output plots; a brief user guide describing the user requirements and options are given in Section III; and an outline of the method of the synthesis analysis in Section IV.

II. Description of the Output Plots

A. Line Plots of ℓn f Iso-Contours (Figure 4).

Two representations of the synthesized distributions are shown in Figure 4. In Figure 4a, the coordinates are the proper frame speed W and pitch angle θ, where $W = |\vec{W}| = |\vec{v}-\vec{u}|$, $\vec{v}$ = electron velocity, $\vec{u}$ = electron bulk velocity averaged over one spacecraft rotation (3 seconds) and θ is the angle between $\vec{W}$ and $\hat{B}$, the symmetry axis. In energy mode 1 or 2, $\hat{B}$ is along the averaged heat flux vector, and its sense is in the earthward hemisphere. In mode 3, $\hat{B}$ is along the magnetic field direction, obtained from the onboard magnetometer. In Figure 4b, the coordinates are the proper speed components, $W_\perp$ and $W_\parallel$, and the plot is required to be symmetric about $W_\perp = 0$.

The solid lines are the iso-contours of ℓn f, successive contours corresponding to variations in ℓn f equal to unity. The dashed lines are the 36 "data tracks" in velocity space along which measurements are made during one spacecraft revolution (6 detectors x 6 angular sectors). In accordance with the gyrotropy assumption, all 36 data tracks have been rotated about the field direction into the same (W, θ) plane and, therefore, some rotated tracks will appear to intersect in this coordinate system as shown in Figure 4. Since the electron plasma is sampled at discrete points in phase space, there will be regions in phase space in which there are no measured points which are filled in by interpolation in order to do the contouring. The interpolation is done in two steps in the (W, θ) representation; first, an interpolation is done over the measured energies along each data track (i.e., each detector and sector) followed by an interpolation over pitch angle. The resulting surface ℓn f as a function of (W, θ) is then smoothed before contouring. The representation in $(W_\perp, W_\parallel)$ coordinates in Figure 4b is obtained by a point-for-point transformation of the smoothed distribution in (W, θ) coordinates in Figure 4a.

B. Gray-Shaded Plots (Figure 5).

The plots in Figure 5a and 5b are the gray-shaded version of the line plots in Figure 4a and 4b, respectively. Line contouring provides better pixel resolution, but gray shading requires less execution time. (The gray shading package used was prepared and documented by M. L. Kaiser and P. G. Harper.) The continuous gray scale is obtained by digitizing $\ell n\ f$ to a scale of integers IZ given by

$$IZ = (\ell nf - (\ell n\ f)\ max + \ell n\ ZG) * NP/\ell n\ ZG$$

where NP = 16 on 12" Versatec plots, and NP = 64 on 22" Versatec plots. The parameter NP, the dynamic range $\ell n\ ZG$, and the maximum, $(\ell n\ f)\ max$, of the $\ell n\ f$ scale may be adjusted as discussed in Section III. The set of integers IZ become the element values of an input array which converts IZ to proportional shades of gray; IZ = NP is blackest, IZ = 0 is whitest. If $\ell n\ f$ exceeds the allowed range, then IZ is set equal to the appropriate bound, IZ = NP or IZ = 0. For a given contrast or difference in gray levels, $\Delta(IZ)$, the corresponding difference in $\ell n\ f$ is $\Delta(\ell n\ f) = (\ell n\ ZG/NP)\ \Delta\ (IZ)$.

The white contours are levels of constant $\ell n\ f$ which are superimposed on the continuous gray scale. The fixed values of gray level at which contours are placed are the set of integers

$$IZ\ (fixed) = IZ/(NP/8),\ IZ = 0\ to\ NP.$$

The difference in gray level between successive contours is $\Delta(IZ) = NP/8$. The corresponding change in $\ell n\ f$ is $\Delta(\ell n\ f) = \ell n\ ZG/8$. For example, if the range of f(v) on the gray scale is set at $ZG = 8.886 \times 10^6$, then between fixed contours $\Delta(\ell n\ f) = (\ell n\ 8.886 \times 10^6)/8 = 16/8 = 2$, or f changes by the factor e^{-2} between contours.

The black bands running more or less vertically in the W -θ grid of Figure 5a outline the data void in the parallel and anti-parallel directions. These are the locations in (W -θ) space of measurements of the

two detectors oriented closest to $\theta = 0°$ and $\theta = 180°$ pitch angle. The region between the outer bands and the edge of the grid, therefore, contain interpolated data only. As will be discussed in Section IV, the interpolation is performed by noting that $f(W_\parallel, W_\perp) = f(W_\parallel, -W_\perp)$, i.e., that f is mirror symmetric about the $\hat{B}$ direction. Thus the interpolation near 0° and 180° is not an extrapolation; rather it is a trend synthesis.

In Figure 5c, the parallel and perpendicular cuts of the smoothed and interpolated ℓn f are plotted as indicated on the plot. Note that these cuts may not be determined by direct measurements in the selected dirction; rather, they are the trend suggested by the closest measurements and the "aperture synthesis" approach adopted here.

Parallel: ℓn $f(W, \theta = 0°)$ is taken from the W -θ grid and plotted as ℓn $f(W_\parallel)$ vs $W_\parallel$ on the right side of the plot. On the left-hand side, ℓn f $(W, \theta = 180°$ is plotted as ℓn f $(-W_\parallel)$ vs $-W_\parallel$.

Perpendicular: ℓn f $(W, \theta = \pi/2)$ is also taken from the W -θ grid and plotted as ℓn f $(W_\perp)$ vs $W_\perp$. The plot is symmetric about $W_\perp = 0$ due to the required symmetry about B.

One-count level: The ℓn f corresponding to the one-count level of the detector is plotted on the same scale as the parallel and perpendicular distribution. It is not a smooth curve since the integration time is not independent of the sampled speed.

Vertical Axis: The scale of ℓn f is from (ℓn f) max to (ℓn f) max -ℓn Z; (ℓn f) max can be the same value as used in the contour plots or it can be a separate fixed value as discussed in Section III. The range of ℓn f, i.e., ℓn Z, is a required input and is discussed in Section III.

In Figure 5d, the coordinates axis are the same as those in Figure 5b. The bottom half plane contains the velocity space locations of the measured data points during one spacecraft revolution. These are the points used in determining the data tracks shown in Figure 4. The upper half plane shows contours of the synthesized distribution function, but without any

smoothing. This plot should be compared with the smoothed plot in Figure 5b to gain an impression of the level of fluctuations in the synthesized distribution and what the effect of smoothing has been. The smoothing used after the interpolation is to preclude the introduction of angular signatures sharper than the angular homogeneity of the analysis system at any given energy, viz., $\theta \sim (4\pi/6 \text{ detectors} \times 6 \text{ sectors})^{1/2} \times 57 = 34$ degrees.

In Figure 5e, the natural logarithm of the reduced distribution function, $\ln F(W_\parallel)$ (vertical axis) is plotted against $W_\parallel$ (horizontal axis). The reduced distribution is given by

$$F(W_\parallel) = 2\pi \int_0^\infty f(W_\parallel, W_\perp)\, W_\perp \, d\, W_\perp .$$

The program computes $F(W_\parallel)$ by integrating the smoothed, un-normalized values of $W_\perp f(W_\parallel, W_\perp)$ from Figure 4b along columns, i.e., over $W_\perp$ at given $W_\parallel$. The $\ln F(W_\parallel)$ is plotted on a scale from $\ln (5 \times 10^{-7})$ to $\ln (5 \times 10^{-15})$, allowing comparisons to be made between various distributions. The horizontal scale is identical to that of Figure 4c.

The Landau damping decrement of plasma oscillations that may be present, $\ln (-\lambda)$ is computed and plotted in Figure 5e as a function of $W_\parallel$. The scale of $\ln (-\lambda)$ is from $\ln (10^3)$ to $\ln (10^6)$. Details of the calculation of $F(W_\parallel)$ and λ are given in the Appendix.

Points for which $\lambda > 0$ are ignored at present. This of course is the interesting case in which a positive slope of $F(W_\parallel)$ results in the growth of plasma oscillations. In a future version of the program, these points could be flagged and included on the same plot as the damping decrement.

The two printed lines at the top of the plot in Figure 5 are selected electron fluid moment parameters averaged over one spin (3 seconds).

First line:
- N = electron density (cm^{-3})
- U = electron bulk speed (km/s) and its GSE X, Y, Z components
- T = temperature (°K)
- A = anistropy, $T_\parallel/T_\perp$.

Second line: H = heat flux (ergs/cm^{2}s) and its
GSE ϕ, θ coordinates

$$S = \text{sign of } \frac{\hat{R} \cdot \hat{X}_{SE}}{H}$$

When S = -1, $\hat{R}$ points toward Earth,
S = +1, $\hat{R}$ points toward the Sun.

The date when the plot was made is at the far right at the top. At the bottom of the plot, the year, decimal day, and UT of the measurement is printed.

III. Using the Contouring Program

A. Required Inputs

The required inputs are the same for the gray-shading and line contour versions and are given below:

JDECDY	= decimal day of year	
JHR	= hours	Day and time (UT) of the start
JMIN	= minutes	of the data interval
JSEC	= seconds	to be processed.

MAPS = total number of spectra (one each spin) to be plotted.

ISKIP = a parameter determining whether consecutive spectra are to be plotted.
For example: ISKIP = 1, every spectra is plotted;
ISKIP = 2, every other one, etc.

The time in seconds spanned by the data interval is MAPS*ISKIP * 9 or MAPS*ISKIP*18 depending on the data format: In format 1, the spectra are 9 seconds apart; in format 2, the spectra are 18 seconds apart.

B. Program Options for the Gray-Shading Version.

Various parameters which control the available options are entered through NAMELIST/INPUT/for the gray version; there are no options for the line contouring version.

1. Plot parameters

Parameter	Function	Default
JPRNT = 0	Various moments computed over individual sectors and spin-averaged are included in printout.	0
= 1	Extended printout lists input data and tabulation of contoured data.	
IZSET = 0	The $f_{\parallel}, f_{\perp}$ plots use default value of scale maximum.	0
= 1	ZMXX will override default value (Note: If IZSET = 1, value of ZMXX must be entered).	
ZMXX	Desired scale maximum of $f_{\parallel}, f_{\perp}$ plot.	1×10^{-24}
IZABS = 0	The $f_{\parallel}, f_{\perp}$ plots are normalized to 1.	
= 1	A fixed scale maximum of $f_{\parallel}, f_{\perp}$ for all plots will be used. The value used depends on IZSET and ZMXX entered above.	1
IFLOW = 0	Plots assume proper frame correction is negligible.	
= 1	Plots are in proper frame coordinates. (*Note: When IMODE = 3, default = 0).	1*
Z	Dynamic range of f on $f_{\parallel}$, $f_{\perp}$ plots	1×10^{7}

ZG	Dynamic range of f covering range of gray scale.	1×10^7

The parameters ZMXX, Z and ZG are R*4 variables; the rest are I*4.

The following examples illustrate some possible plot options:

a) Change nothing: If only default values are used, then ZG = 1×10^7, Z = 1×10^7 and (f) max on $f_\parallel, f_\perp$ plot will be 5×10^{-25} for modes 1 and 2, and 3×10^{-28} for mode 3.

b) To specify range of f on contour plot: change ZG.

c) To specify range of f on $f_\parallel$, $f_\perp$ plot: change Z.

d) To specify f max on $f_\parallel, f_\perp$ plot: set IZSET = 1 and specify ZMXX.

e) To normalize $f_\parallel, f_\perp$ plot to 1: set IZABS = 0.

2. Additional parameters

The following parameters controlling output have been added to NAMELIST/INPUT/:

Parameter	Function
KPRNT ≠ 0	The values of in f on the (W,θ) grid may be printed out at various steps in the syntnesis analysis. (See the current listing for details.)
	Default: KPRNT = 0
ITAP ≠ 0	The reduced distribution function as a function of parallel proper velocity is written out on tape.
	Default: ITAP = 0

3. Symmetry axis

In the current version of the gray-shading package, the symmetry axis with unit vector components B(I), I = 1,3 (GSE Cartesian coordinates) may be taken to be along either 1) the electron heat flux vector direction with its sense earthward, or 2) along another specified direction parallel to the vector with components BF(I), I = 1,3. The parameter controlling the users option is IBEXT and is entered through NAMELIST/INPUT/. The options are as follows:

Parameter	Function
IMODE = 1 or 2 IBEXT = 0	The symmetry vector B is along the electron heat flux vector but in the earthward sense.
IMODE = 3 IBEXT ≠ 0	The symmetry vector B is along the normalized BF direction, where BF is the 5 min average of the magnetic field obtained from the ISEE-1 magnetic field experiment and is read from the input tape to this program along with the electron plasma data.
IMODE = 1,2, or 3 IBEXT ≠ 0	Any symmetry vector could be specified by entering BF(I) I = 1,3, through an additional input which overrides the input magnetic field when in IMODE = 3. The required additional input is not now a part of the program, but the necessary branching for this option is in place.
	Default: IBEXT = 0

4. Smoothing Parameters

The remaining control parameters that may be changed through NAMELIST/INPUT/ are ISZY, NC, NH, WC, WH. These parameters control the

size of the smoothing interval in pitch angle and speed. It is not necessary to enter them as inputs since they have default values. These parameters and the smoothing are described in Section IV-E.

B. Job Submittal

The following sequence of JCL statements and data are required to run the program on the 360/91. Decks are available on request.

1. Gray-shading version.

```
00100 // EXEC LOADER,REGION=499K,PARM='SIZE=495K,EP=MAINIS,LET'
00110 //SYSLIB DD DSN=M2.U3MLK.LODMOD,DISP=SHR
00120 //        DD DSN=SYS1.MOD2.FORTLIB,DISP=SHR
00130 //SYSLIN DD
00140 //        DD DSN=SYS2.LOADLIB(U3RJFGR1),DISP=SHR
00141 //GO.FT06001 DD SYSOUT=B,DCB=(RECFM=VBA,LRECL=137,BLKSIZE=1789)
00142 //GO.FT08F001 DD DUMMY,SYSOUT=A,DCB=(RECFM=VBA,LRECL=137,BLKSIZE=1789)
00150 //GO.FT10F001 DD DSN=ISEEA.SUMMARY,LABEL=(,SL,,IN),
00160 // DCB=(RECFM=VS,BLKSIZE=14056,LRECL=14052,DEN=4,OPTCD=B,BUFNO=1),
00170 // VOL=SER=FP8804,DISP=(SHR,KEEP),UNIT=(6250,,DEFER)
00180 //GO.FT20F001 DD UNIT=800,LABEL=(1,NL,,OUT),
00190 //   DSN=REDUCE,DCB=(RECFM=F,BLKSIZE=4745,LRECL=4745,DEN=2,OPTCD=Q),
00200 //   DISP=(MOD,KEEP),VOL=SER=FP8721
00210 //DATA5 DD *
00220  &INPUT IZABS=1,Z=1E7,ZG=1E7,IZSET=1,ZMXX=1E-24,JPRNT=0,KPRNT=0,&END
00221 311 02 11 00 01 01
00280 //VPLOT    DD UNIT=800,DCB=DEN=2,LABEL=(,NL),
00290 //   VOL=SER=TD5054
00300 // EXEC NTSO
```

Lines 150-170:	Input tape DD statement.
Lines 180-200:	Optional output tape DD statement (See Section III B.2).
Line 220:	NAMELIST/INPUT/ containing parameters controlling program option.
Line 221:	Data interval JDECDY, JHR, JMIN, JSEC, MAPS, ISKIP in the format I3, 5(1X,I2).
Lines 280-290:	Output plot tape DD statement.

Approximate execution time: 10 sec CPU, 1 sec IO

2. Line plot version.

```
00010 // EXEC LINKGO,REGION=499K,PARM='LET'
00020 //SYSLIB DD DSN=SYS2.WOLF.VERSATEC,DISP=SHR
00030 //        DD DSN=SYS2.WOLFPLOT,DISP=SHR
00035 //        DD DSN=SYS2.IMSLS,DISP=SHR
00036 //        DD DSN=SYS1.FORTLIB,DISP=SHR
00037 //        DD DSN=SYS2.FORTLIB,DISP=SHR
00040 //OBJECT DD *
00050   INCLUDE LOADLIB(U3RJFLIN)
00060   INCLUDE SYSLIB(IEVMAP)
00070   ENTRY DFCN2R
00080 //GO.FT08F001 DD DUMMY,SYSOUT=A,DCB=(RECFM=VBA,LRECL=137,BLKSIZE=1789)
00090 //GO.FT10F001 DD DSN=ISEEA.SUMMARY,LABEL=(,SL,,IN),
00100 // DCB=(RECFM=VS,BLKSIZE=14056,LRECL=14052,DEN=4,OPTCD=B,BUFNO=1),
00110 // VOL=SER=FP7877,DISP=(SHR,KEEP),UNIT=(6250,,DEFER)
00120 //PLOTLOG DD SYSOUT=A
00130 //VECTR1 DD DSN=&&VECTR1,UNIT=SYSDA,DISP=(,PASS),SPACE=(TRK,(1,1))
00140 //VECTR2 DD DSN=&&VECTR2,UNIT=SYSDA,DISP=(,PASS),SPACE=(CYL,(1,1))
00150 //DATA5 DD *
00160  &INPUT WX=1,,,5,1,,,5,FLD=2,,2,,1,,1,,&END
00170 312 12 33 00 01 01
00180 // EXEC PGM=IEVMAPP,COND=(EVEN),REGION=300K
00190 //STEPLIB DD DSN=SYS2.WOLF.VERSATEC,DISP=SHR
00200 //PLOTLOG DD SYSOUT=A
00210 //VECTR1 DD DISP=(OLD,DELETE),DSN=&&VECTR1
00220 //VECTR2 DD DISP=(OLD,DELETE),DSN=&&VECTR2
00230 //RASTTAPE DD UNIT=800,DCB=DEN=2,LABEL=(,NL),
00240 //   VOL=SER=TD5060
00250 // EXEC NTSO
```

Lines 90-110:	Input tape DD statement.
Line 170:	Data interval JDECDY, JHR, JMIN, JSEC, MAPS, ISKIP in the format I3, 5(1X,I2).
Lines 230, 240:	Output plot tape DD statement.

Approximate execution time: 45 sec CPU, 1 sec IO.

IV. Method

This section outlines the method of synthesizing the discrete measurements of the distribution function in three dimensions into an array of continuous values which can be contoured. Only the essential steps of the analysis are outlined here; the details are found in the documented computer code which is available upon request. The parts of the computer code that are relevant to this outline can be identified by comments in the code corresponding to the subheadings found here.

A. Read input data.

1. Read the control parameters (explained in Section III).
2. Read the header record containing physical characteristics of the detector which are used in computing the one-count phase density for the given mode of detector.
3. Read the start time of the data interval and the number of records to be processed.
4. Read the data records in the data interval and process one record at a time. The essential data that are read are:

IYR,IDECDY,IHR,MIN,SEC	- Date and time of start of data interval,
CC(J), J = 1, INSET	- Array of speeds corresponding to the tuned energy of spectra, in order of decreasing magnitude,
CNTS(J,L,IS)	- Electron counts,
FBLOK(J,L,IS)	- Phase density of electrons,

where J is the velocity index and L,IS are the detector and sector indices, respectively.

IMODE	- Energy mode.
SPINP	- Spin period

Various moments of the distribution function computed for each sector and averaged over spin are also read.

B. Compute the azimuth in spin plane of the look direction of each detector in each sector.

PHIZ(L,IS) = (360/SPINP)*CYCLT*(IS-1)+DPHI(L)±90 for IS = 1, 6,

where SPINP = updated spin period
CYCLT = sector time
DPHI(L)±90 are the detector azimuths relative to the sector and since DPHI(1) = DPH(6), DPMI(2) = DPHI(5), and DPHI(3) = DPHI(4), the azimuths DPHI(L) ± 90° are 180° apart for the detectors in each of the pairs (1,6), (2,5), and (3,4). For L = 1,2, or 3, the lag is -90°; for L = 4,5,6, the lag is +90°.

C. Choose the axis of symmetry.

When IMODE = 1 or 2, the symmetry axis $\hat{B}$ is along the heat flux direction $\hat{H}$. The sense of $\hat{B}$, however, is chosen always to be directed toward the earthward hemisphere. Therefore when $\vec{H}$ points toward the earth and away from the sun, $\hat{B} = \vec{H}/H$; when $\vec{H}$ points away from the earth, $\hat{B} = -\vec{H}/H$. When IMODE = 3, the symmetry axis must be provided independently of the electron data. (See Section III.B.2).

D. Transform velocity space from the S/C frame to the proper frame of the electrons with $\hat{B}$ as the axis of symmetry.

1. Form the array V(I),I = 1,NV, of the measured speeds from the input array CC. The V array is ordered according to decreasing magnitude.

2. Order the measured speed array, V, and sample time array, TIM, according to increasing velocity magnitude and name them VS(I) and Y(I), respectively. Compute the interpolating spline over Y(time) as a function of VS (velocity magnitude). See Figure 6a.

3. Clear the plotting arrays.

4. For given detector and sector indices, L and IS, eliminate array elements having zero or negative (i.e., "fill") electron counts and form the new arrays

TP(I) = time
YP(I) = log e of the distribution function (ln f)
VP(I) = measured velocity magnitude
I = 1,NV

These arrays are ordered according to decreasing velocity magnitude.

5. Order the arrays TP,YP, and VP according to increasing speed, forming the new arrays

T(I) = time
B2(I) = ln f
B1(I) = measured veleocity magnitude
I = 1,NV

Compute the interpolating spline over B2(ln f) vs. B1 (speed) for given detector and sector corresponding to indices L and IS, respectively. See Figure 6b.

6. The transformation and interpolation

In order to contour ln f measurements, the data are transformed to a regularly spaced grid in the proper frame coordinates W,θ where W is the proper frame speed and θ is the pitch angle relative to the symmetry axis B. This is done by choosing values of W' and, by iteration, finding values of $(V(t), \theta_{SE}(t), \phi_{SE}(t))$ that satisfy

$$(W')^2 = W_x^2 + W_y^2 + W_z^2$$

which, using $\underline{W}$ detected = $\underline{V}$ detected $-\underline{U}_{Bulk}$, may be written in components as

$$W_x = -V(t)\ \sin\theta_{SE}(t)\ \cos\phi_{SE}(t) - U_x$$

$$W_y = -V(t)\ \sin\theta_{SE}(t)\ \sin\phi_{SE}(t) - U_y$$

$$W_z = -V(t)\ \cos\theta_{SE}(t) - U_z$$

(Notice that θ, ϕ are the "look" angles rather than the acceptance angles of the collected flux $\underline{V}_{look} = -\underline{V}_{detected}$.) Since V(t) and $(\theta(t), \phi(t))_{SE}$ depend on one another because of the timing sequence through the energy channels and the spin rate of the S/C, values of V and $(\theta,\phi)_{SE}$ used in the iterative process, must be consistent with the functional relation shown in Figure 6a for V(t) and with

$$\theta_{SE}(t) = \text{THETA(L)} = \text{const for given L}$$
$$\phi_{SE}(t) = \text{PHIZ(L,IS)} + (360/\text{SPINP})*t.$$

Using the computed spline over V(t) in Figure 6a, the value of $t = t'$ and hence $V = V'$ that yields the desired W' is found, and the pitch angle θ' is then given oy

$$\theta' = \cos^{-1}\ \frac{W_x B_x + W_y B_y + W_z B_y}{W'} \ .$$

Ambiguity in $\cos^{-1}$ is irrelevant because of gyrotropy and, therefore, the principle range is 0 to π. The correspondiing value of $\ln f'$ at $V = V'$ is then found using the spline over $\ln f$ vs V given in Figure 6b.

The result of transforming the velocity coordinates of the measurement from the single detector and sector given in Figure 6b is shown in Figure 6c. This data "track" has data points at every horizontal grid line (values of W) which in general, don't fall at the intersections of the vertical grid lines (values of θ_p). After all 36 data tracks have been transformed, intersections of all the tracks with a given horizontal grid

line are used to compute an interpolating spline to find $\ln f$ at each of the 121 grid points on the given horizontal line. Figure 6d illustrates this horizontal interpolation. The entire grid is filled by repeating the procedure for all 60 horizontal grid lines. The interpolation is performed in subroutine INTRP3. This completes the synthesis of the measurements in the (W,θ) space.

A cautionary comment is in order regarding the horizontal interpolation. Note in Figure 6d that the intersections of the 36 data tracks with any given horizontal line are unevenly spaced, being widely separated in some places and crowded or overlapping in others. Since the interpolating spline fitting $\ln f$ vs θ_p will pass through every point on the line, those points that tend to overlap in θ may cause the spline to ring. This can lead to spurious interpolated values depending on how large the gap is between the overlapping points and the nearest neighboring points along the line. The approach to this problem is to average together the points in a given row into 6 degree pitch angle bins before doing the interpolation. This irreducible bin size is fundamental and determined by the field of view of the sensors which is 8.5 x 11 degrees in solid angle. The synthesis therefore reflects solid angle averages which this finite solid angle implies.

The data gap which is usually largest is at the edges of the $W-\theta$ grid near $\theta = 0°$ and $\theta = 180°$, resulting from the fact that the magnetic field is usually close to being in the ecliptic plane when in the solar wind while no detector views the sun directly. To fill this gap with interpolated data and to minimize ringing effects, the spline begins and ends outside the space of interest, i.e., outside the space $\theta = 0°$ to $180°$. This is done by reflecting the half-space between $\theta = 90°$ to $0°$ about $\theta = 0°$ and reflecting the half-space between $\theta = 90°$ to $180°$ about $\theta = 180°$. This is consistent with the assumption of cylindrical symmetry. Therefore, these gaps are filled with interpolated data and are <u>not</u> an extrapolation. Note that in the absence of any tendency for iso-contours of $\ln f$ to slope, then the <u>de facto</u> interpolation across the data gaps at $0°$ and $180°$ will be contours which are straight lines in (W,θ) space and circles in $(W_\perp, W_\parallel)$ space. Therefore if the synthesis suggests non-circular deformation at $0°$ and $180°$, it must reflect contours with $\partial f/\partial\theta \neq 0$.

E. Smoothing the interpolated data.

Before contouring the ℓn f data on the filled W -θ grid, a two variable smoothing function S(W,θ) is used. The characteristics of S(W,θ), which slides over the grid, are sketched in Figure 7. Since the channel separation varies with speed, the width along W is variable, being wider at higher speeds. The parameters ISZY,WC,WH,NC, and NH are adjustable through NAMELIST (see Section IV) in the gray-shaded version. In the line plot version, these parameters are fixed and equal to the default values of the gray-shaded version. The default values are:

ISZY = 1. (a R*4 variable)
NC = 10 units of pitch angle (1 unit = 1.5 degrees) = 15 degrees
NH = NC
WC = 1., WH = 0.4

Thus the core of the default S(W,θ) is 30° wide and is flat in amplitude; the wings extend 15° on either side with reduced amplitude.

This choice of smoothing function was based on the following considerations:

a) Coarseness in the data is introduced by the two-way interpolation as discussed above.

b) The size of the smoothing window in the θ dimension should not be finer than the degree of continuity that is implied by sampling f(Ψ) in 36 discrete directions over 4π steradians at a given energy during one spacecraft rotation. An estimate for that average spacing in angle is $(4\pi/36)^{1/2} \approx 57$ degrees = 34 degrees.

c) The computation must be economical in computer time. This is why the smoothing function was constructed using flat segments.

F. Transformation from (W, θ) to ($W_\perp$, W_n) coordinates.

The smoothed data on the (W, θ) grid are transformed to the (W_n,$W_\perp$) grid with no additional smoothing. A two-dimensional interpolation is used as follows:

$$G^{-1} \times \ln f(W_n,W_\perp) =$$
$$(W'-W_i)\,[(\theta'-\theta_i)\ln f(\theta_{i+1},W_{i+1}) + (\theta_{i+1}-\theta')\ln f(\theta_i,W_{i+1})] +$$
$$(W_{i+1}-W')\,[(\theta'-\theta_i)\ln f(\theta_{i+1},W_i) + (\theta_{i+1}-\theta')\ln f(\theta_i,W_i)]$$

Where W_n,$W_\perp$ is a point at an intersection of grid lines, W',θ' is the corresponding point on the (W, θ) grid, $W' = W_n^2 + W_\perp^2$, and $\theta' = \cos^{-1}(W_n/W')$. The constant $G = (W_{i+1} - W_i)(\theta_{i+1} - \theta)$.

The point (W', θ') is not at a grid intersection, in general, but falls within the box whose corners are (W_i,θ_i), (W_{i+1},θ_i), (W_i,θ_{i+1}), and (W_{i+1},θ_{i+1}). The interpolated value contains contributions from the value of ln f at all four corners weighted by the inverse of the distance of the point (W',θ') from each corner.

The full polar plot in Figure 4 and Figure 5 is obtained by reflecting the plot about $W_\perp = 0$, i.e.,

$$\ln f(W_n,-W_\perp) = \ln f(W_n, W_\perp).$$

REFERENCES

Kaiser, M. L. and P. G. Harper, Manual for Code 690 users of the Versaplot system and the gray shading package, 1980.

Ogilvie, K. W., J. D. Scudder, and H. Doong, The electron spectrometer experiment on ISEE-1, IEEE Trans. on Geo. Electr., GE-16, 261, 1978.

FIGURE CAPTIONS

FIGURE 1 (a) Velocity space coverage of the experiment. (b) Timing diagram for the electron energy spectrum measurement.

FIGURE 2 Measurements of the velocity distribution function by the ISEE VES experiment during one complete spin of the spacecraft. The data in each sector is acquired in 0.5 seconds, the three pairs of opposed sensors being sampled simultaneously in each energy channel. These 576 discrete measurements are distributed throughout phase space due to the timing of the energy steps as the spacecraft goes through one complete rotation.

FIGURE 3 (a) Line-contour plot of the synthesis of the discrete measurements of the distribution function shown in Figure 2. The velocities, $W_\perp$ and $W_\parallel$, are the speeds perpendicular and parallel to the magnetic field in the frame moving with the electron bulk flow. Cylindrical symmetry about the parallel direction is assumed. (b) Gray-shaded version of contour plot showing gradual changes in the distribution function. The white lines are contours at fixed values of $f(\vec{W})$.

FIGURE 4 Output of the line contour plot package. See text.

FIGURE 5 Output of the gray-shaded plot package. See text for detailed explanation.

FIGURE 6 (a) Timing sequence of the velocities at which the distribution function is sampled at each detector in each sector. (b) Measured values of log e of the distribution function, $\ln f$, at a particular detector (L = 1) and sector (IS = 1). By fitting splines to the data in (a) and (b) points are filled in by interpolation on this phase space track and represented in proper frame coordinate speed and pitch angle, as in (c) The location of all 36 data tracks

during a complete rotation are shown in (d). The points along each track are chosen to intersect horizontal grid lines, but, in general do not intersect at vertical grid lines. The values of ln f and pitch angle at the horizontal grid intersections (shown for one horizontal grid line) are used to interpolate at the intervening vertical grid intersections. The grid size is 60 (speed) by 120 (pitch angle).

FIGURE 7 The two-dimensional smoothing function that slides over the W,θ grid, smoothing the values of ln f filled in by the two way interpolation (see text).

APPENDIX: Calculation of the reduced distribution function and the Landau damping decrement.

The reduced distribution function $F(W_\parallel)$ that is plotted in Figure 5e is defined as

$$F(W_\parallel) = 2\pi \int_0^\infty dW_\perp \, W_\perp \, f(W_\parallel, W_\perp) \qquad \text{A1}$$

where $W_\parallel$ and $W_\perp$ are the parallel and perpendicular proper frame velocites, respectively, and $f(W_\parallel, W_\perp)$ is the smoothed, synthesized gyrotropic distribution functions in the $W_\parallel$, $W_\perp$ velocity space as shown in Figure 5b. The precise limits of integration can extend only over the range of sampled data, W_{min} to W_{max}. However, the contribution to the integral outside the sampled range of velocities can be approximated with help of the following change of variable:

$$X = \frac{W_\perp - W_{min}}{W_{th} + W_\perp - W_{min}}$$

$$Y = \frac{(W_{th} + W_\perp - W_{min})^2}{W_{th}} \; W_\perp \, f(W_\parallel, W_\perp), \qquad \text{A2}$$

where W_{th} = is estimated thermal speed. Then, $\int_{W_{min}}^{W_{max}} dW_\perp \, W_\perp \, f(W_\parallel, W_\perp) =$

$$\int_0^{X_{max}} Y \, dX.$$

Extending the lower integration limit to zero, $W_{min} = 0$, can be done by noting that the integrand vanishes, i.e., $Y \propto W_\perp \, f(W_\parallel, W_\perp) = 0$ at $W_\perp = 0$.

The upper integration limit can be extended to $W_{max} = \infty$ by noting that $X_{max} \to 1$ as $W_{max} \to \infty$ and assuming that $f(W_\parallel, W_\perp)$ falls off faster than $W_\perp^{-3}$. Therefore

$$F(W_n) = 2\pi \int_0^1 dx\, Y. \qquad A3$$

The variables X and Y are given by Equation A2 and the integral is calculated by an n-point trapezoidal formula. The set of (X_i, Y_i) for i = 2, n-1 are taken from points along a vertical grid line at given θ, in the $W_\perp$, W_n representation of Figure 4b or Figure 5b. The end points are $X_1 = 0$, $Y_1 = 0$ and $X_n = 1$, $Y_n = 0$, corresponding to $W_\perp = 0$ and $W_\perp = \infty$, respectively.

The Landau damping decrement, W_i, is computed as follows (Krall and Trivelpiece, page 520):

$$\omega_i = -\frac{\pi}{2}\frac{\omega_{pe}^2}{k^2}\omega_r \left.\frac{\partial F(W_n)}{\partial W_n}\right|_{W_n = \frac{\omega}{|k|}} \qquad A4$$

where ω_{pe} = electron plasma frequency, k = wave number, and ω_r = real part of the electron plasma wave frequency.

If we set $\omega_{pe}^2/k^2 = W_n^2$ and $\omega_r = \omega_{pe} = 2\pi\, 10^4\, (n_e)^{1/2}$, where n_e = electron density (cm^{-3}), then,

$$\omega_i = -\frac{\pi}{2} W_n^2\, \omega_{pe}\, F\, \frac{\partial \ln F}{\partial W_n}$$

$$= -\pi^2\, 10^4\, n_e\, W_n^2\, F\, \partial \ln F/\partial W_n \qquad A5$$

Equation A5 is used to compute and plot in Figure 5e the plasma wave damping decrement ω_i as a function of W_n. The plot of ω_i for all W_n does not imply that plasma waves are necessarily present at all wave velocities, but rather, that if waves are present, then the damping effect of this electron distribution would be given by Equation A5. Points are excluded

from the plot which correspond to wave growth, i.e., when $\partial \ln F/\partial W_n > 0$.

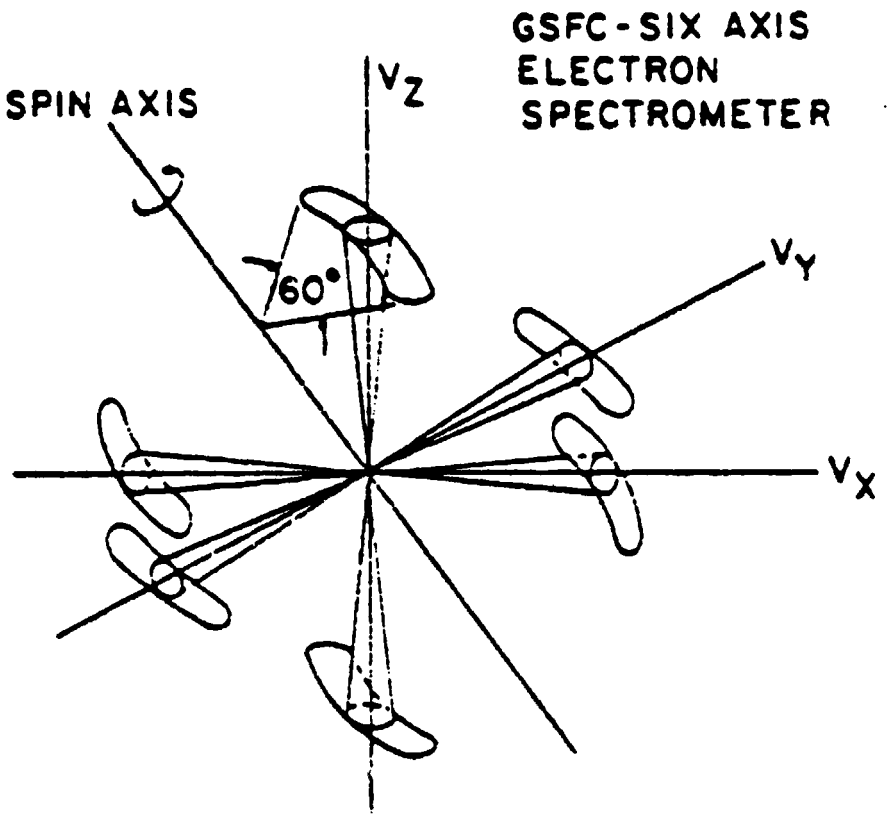
GSFC-SIX AXIS
ELECTRON
SPECTROMETER
SPIN AXIS
V_Z
60°
V_Y
V_X

(a)

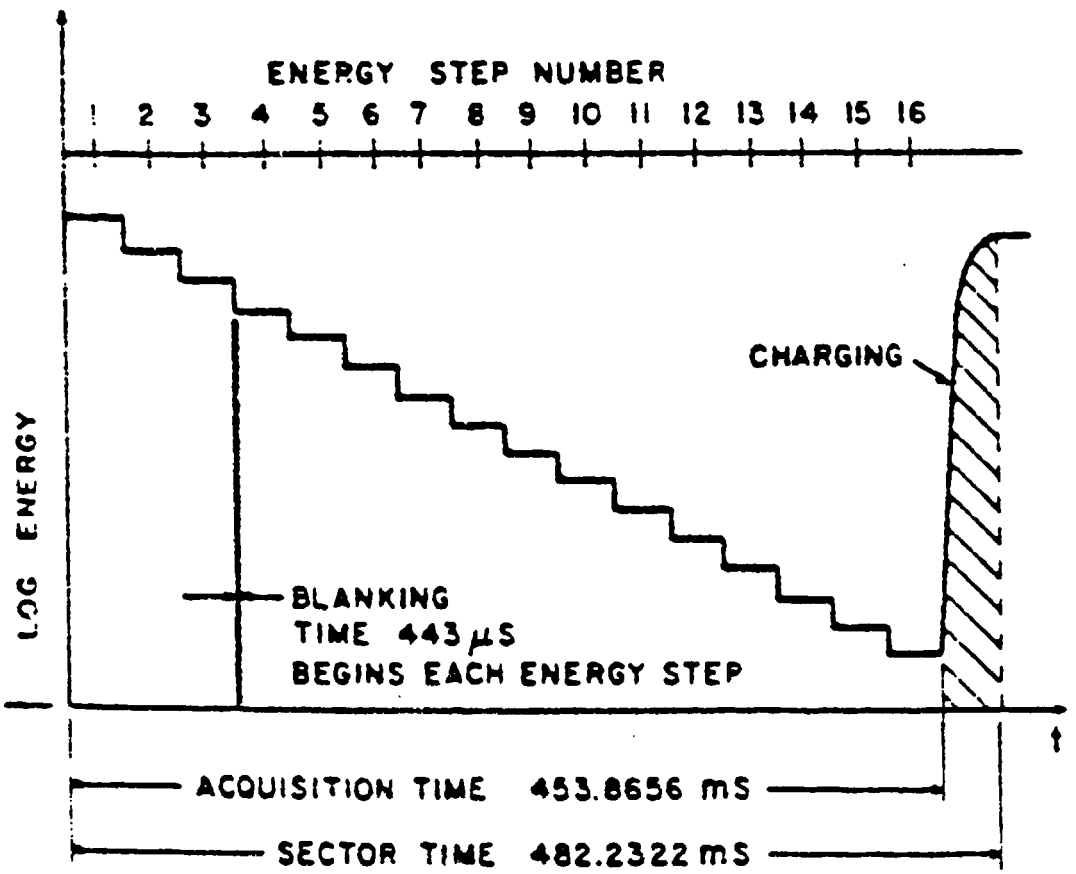
ENERGY STEP NUMBER
1 2 3 4 5 6 7 8 9 10 11 12 13 14 15 16
LOG ENERGY
CHARGING
BLANKING
TIME 443 μS
BEGINS EACH ENERGY STEP
t
ACQUISITION TIME 453.8656 mS
SECTOR TIME 482.2322 mS

(b)

Figure 1

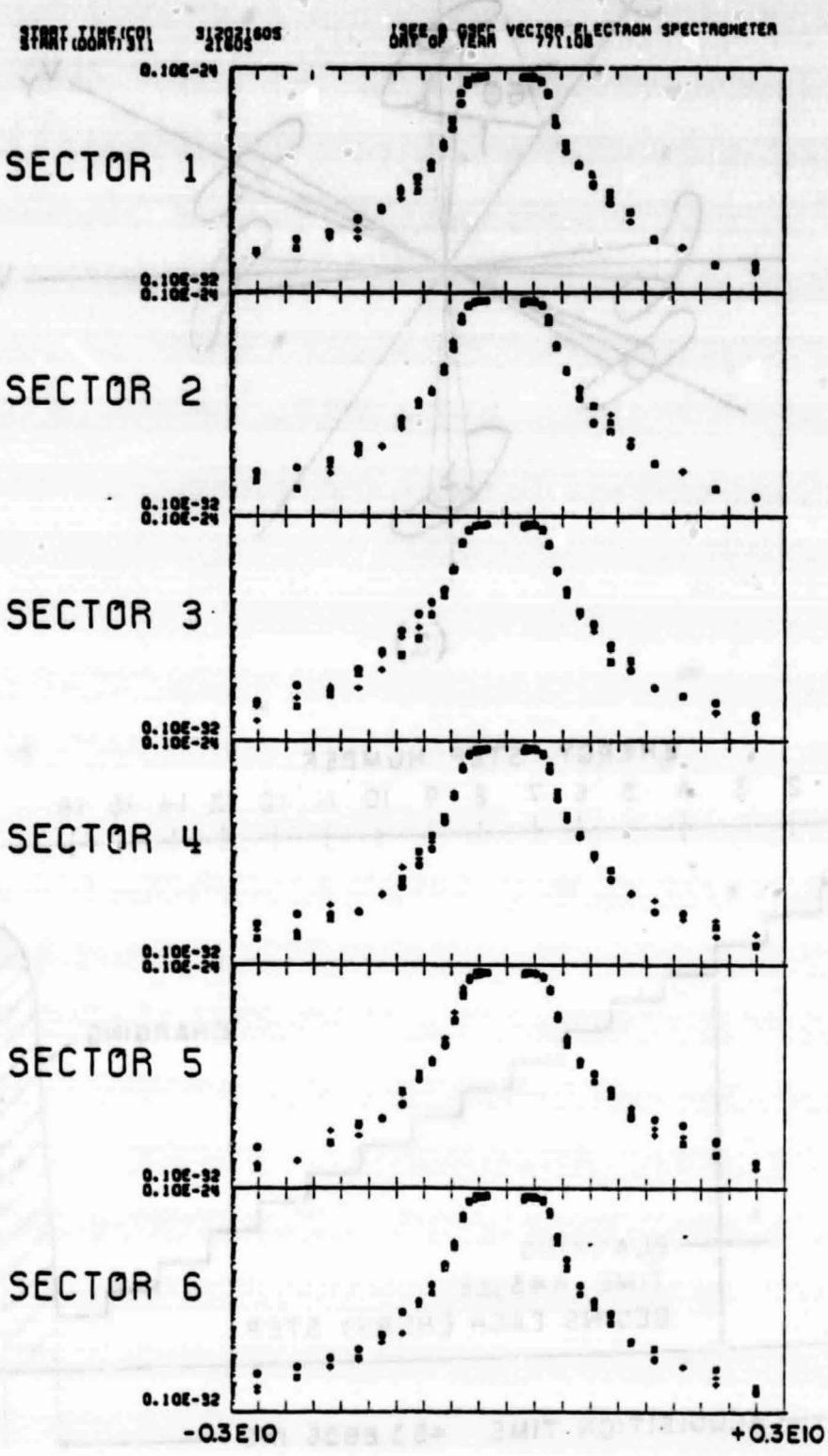
VECTOR ELECTRON SPECTROMETER
SECTOR 1
SECTOR 2
SECTOR 3
SECTOR 4
SECTOR 5
SECTOR 6
0.10E-24
0.10E-32
-0.3E10
+0.3E10

Figure 2

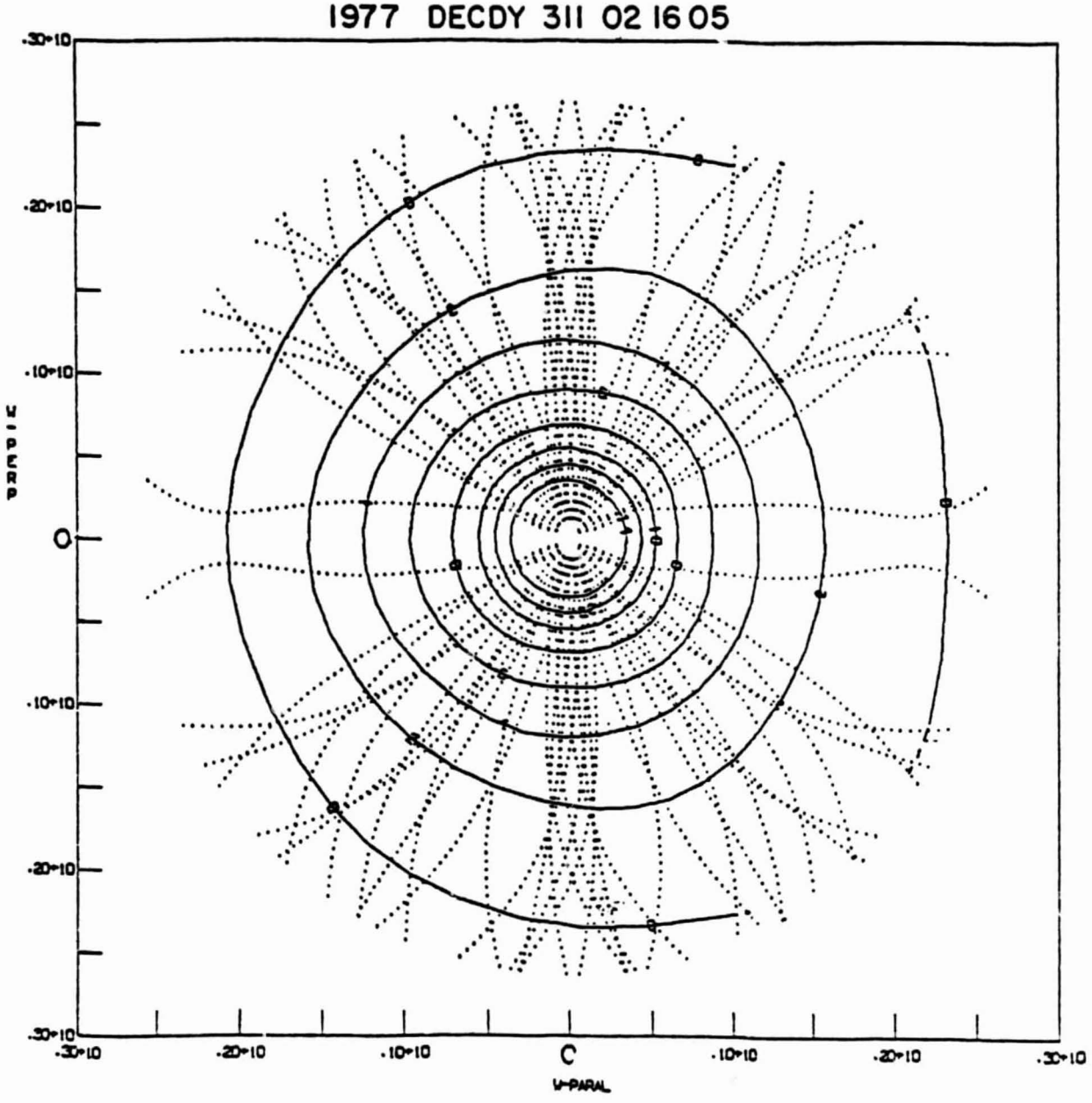
1977 DECDY 311 02 16 05
.30+10
.20+10
.10+10
0
.10+10
.20+10
.30+10
PERP
.30+10
.20+10
.10+10
C
.10+10
.20+10
.30+10
V-PARAL

Figure 3a

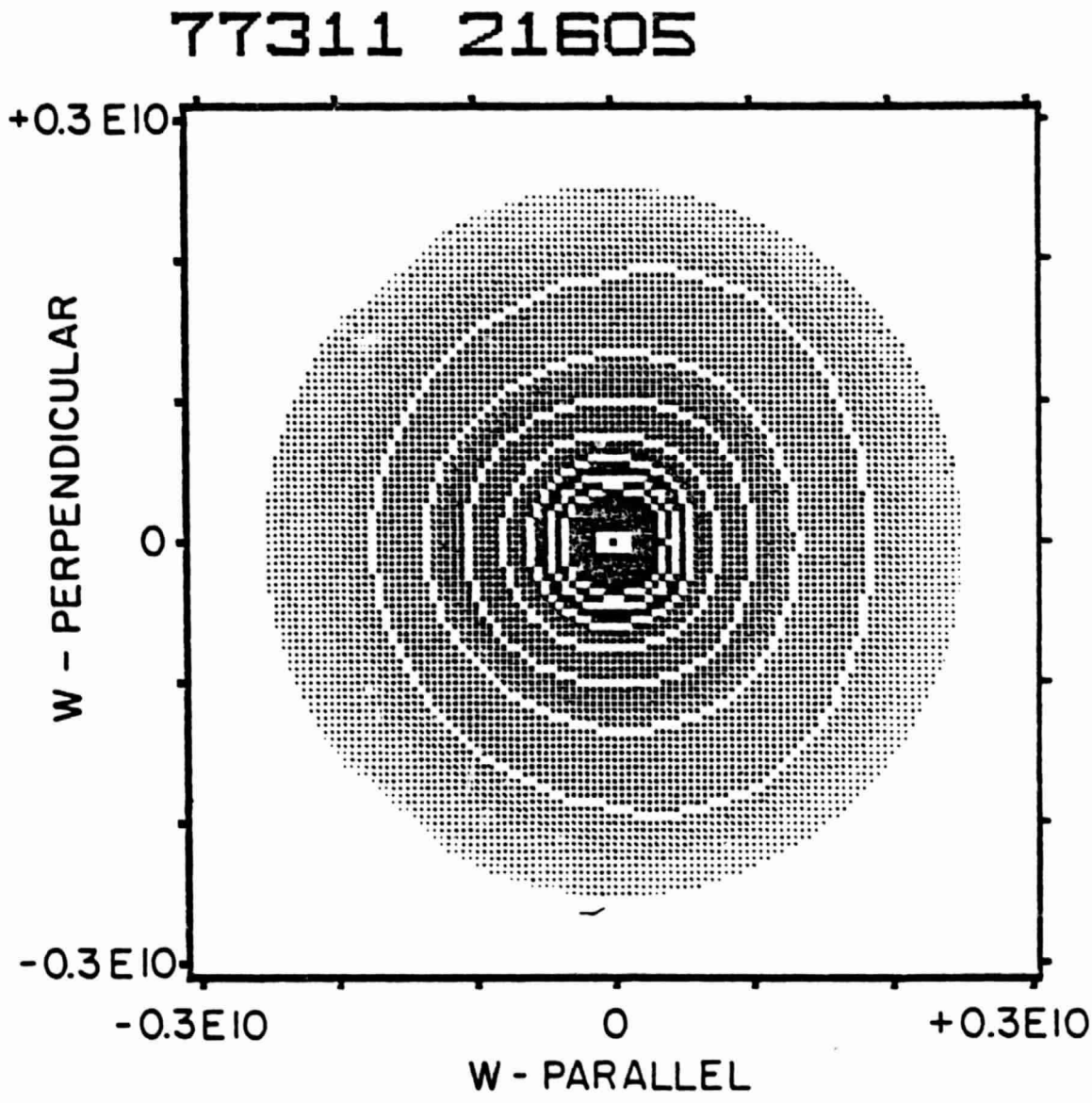
77311 21605
+0.3 E10
0
-0.3 E10
W - PERPENDICULAR
-0.3E10
0
+0.3E10
W - PARALLEL

Figure 3b

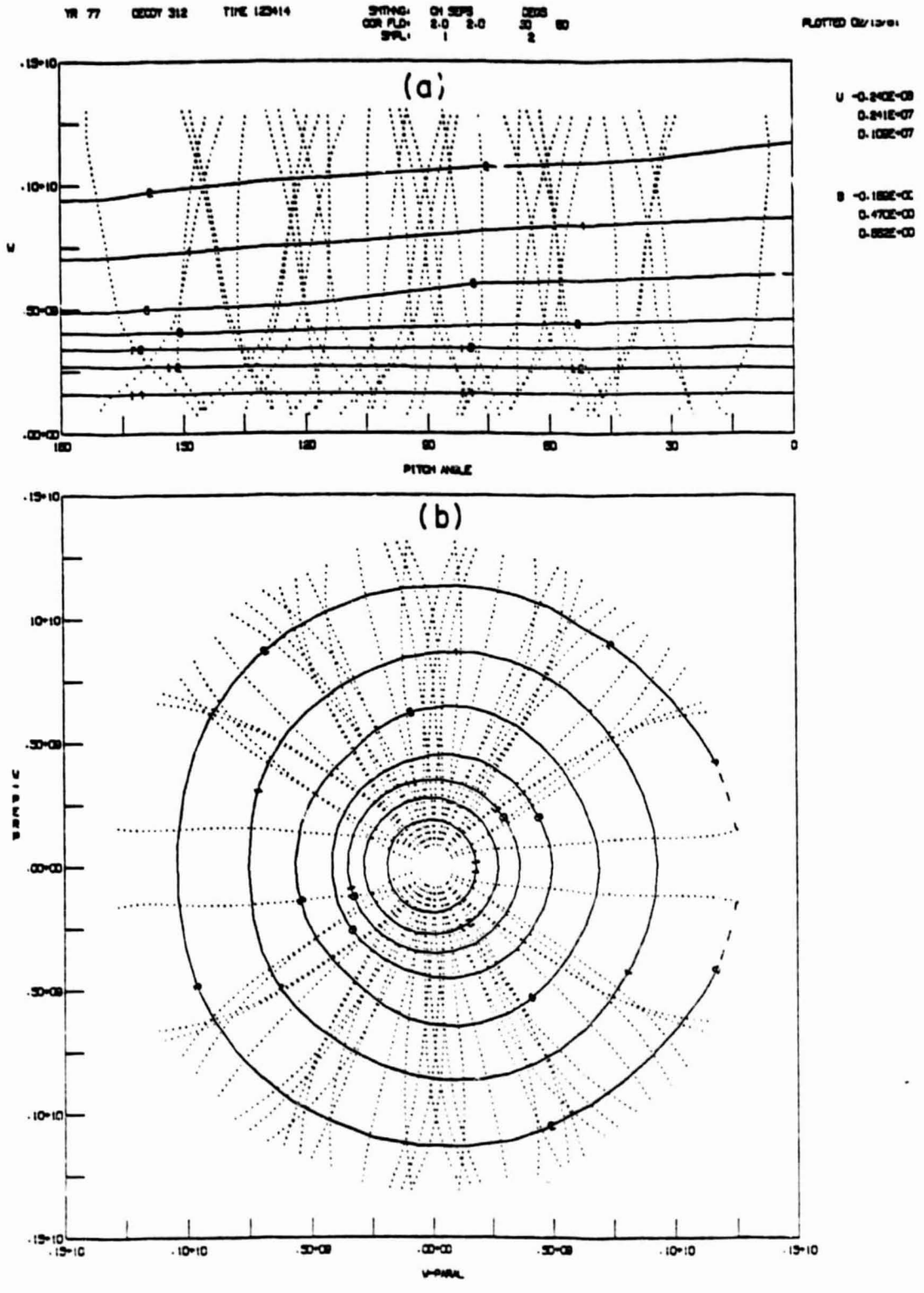

Figure 4

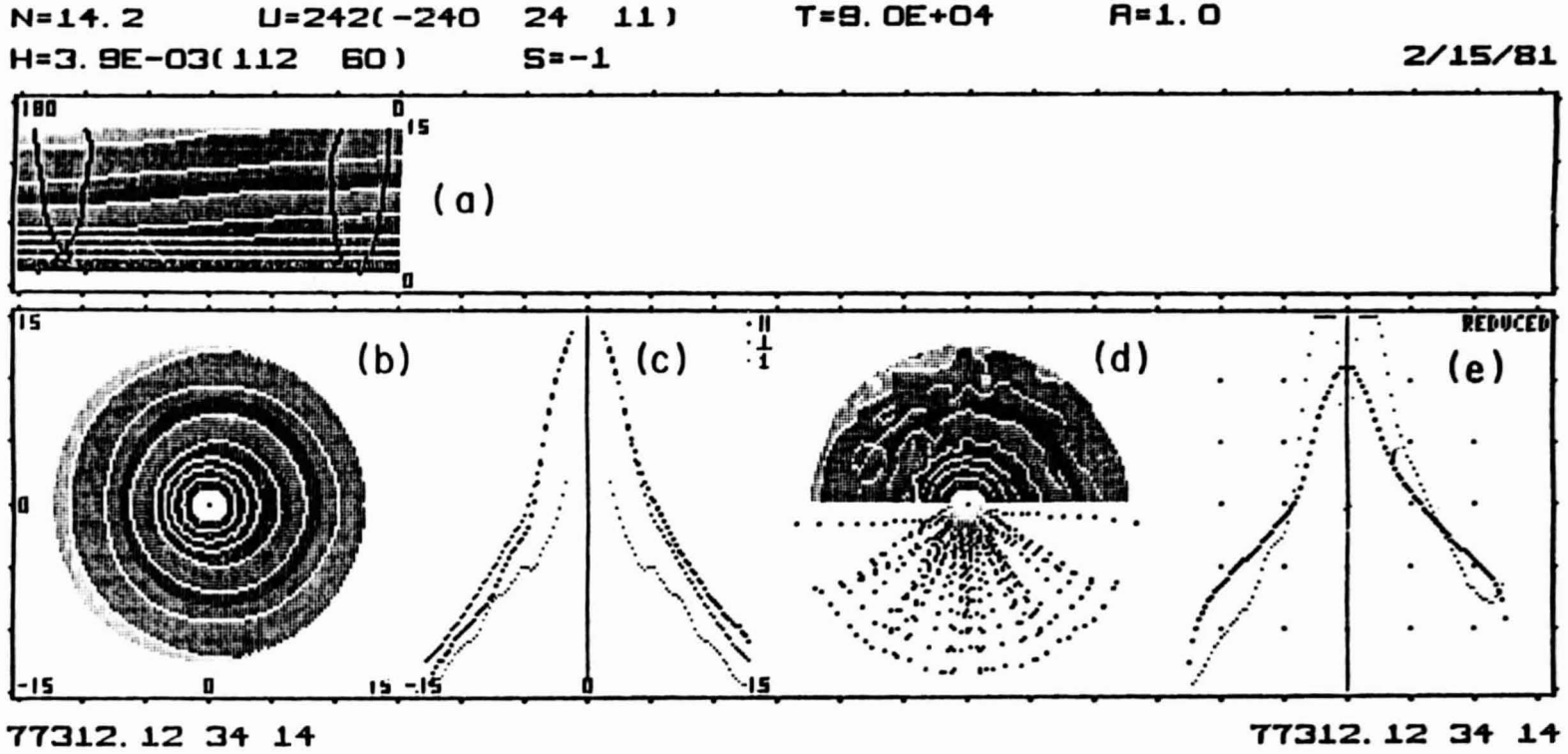
N=14.2 U=242(-240 24 11) T=9.0E+04 A=1.0
H=3.9E-03(112 60) S=-1 2/15/81
180
0
15
0
(a)
15
0
-15
0
15
-15
(b)
(c)
(d)
(e)
REDUCED
77312.12 34 14
77312.12 34 14

Figure 5

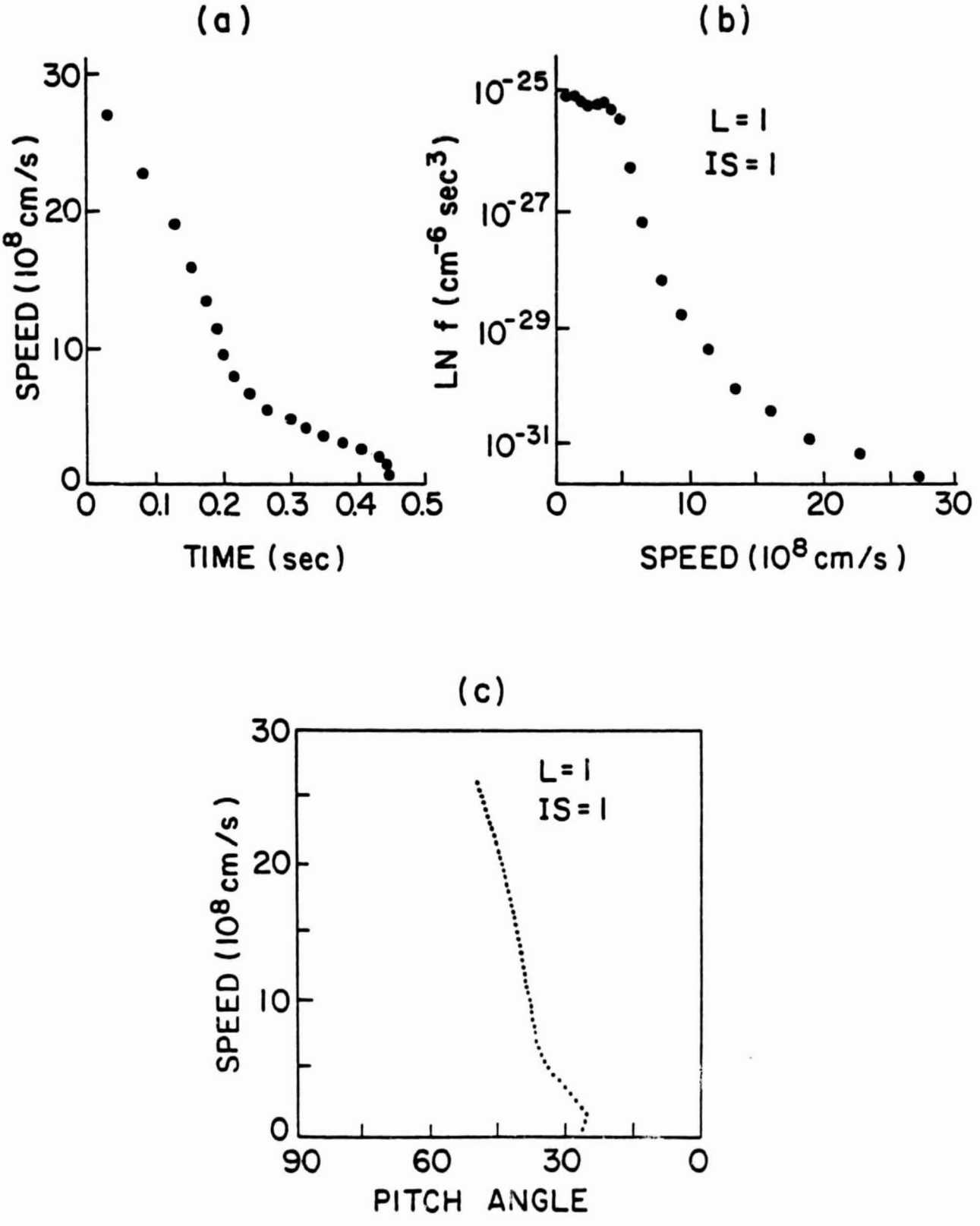
(a)
SPEED (10^8 cm/s)
30
20
10
0
0
0.1
0.2
0.3
0.4
0.5
TIME (sec)
(b)
LN f (cm^{-6} sec^3)
10^{-25}
10^{-27}
10^{-29}
10^{-31}
L = 1
IS = 1
0
10
20
30
SPEED (10^8 cm/s)
(c)
SPEED (10^8 cm/s)
30
20
10
0
L = 1
IS = 1
90
60
30
0
PITCH ANGLE

Figure 6a-c

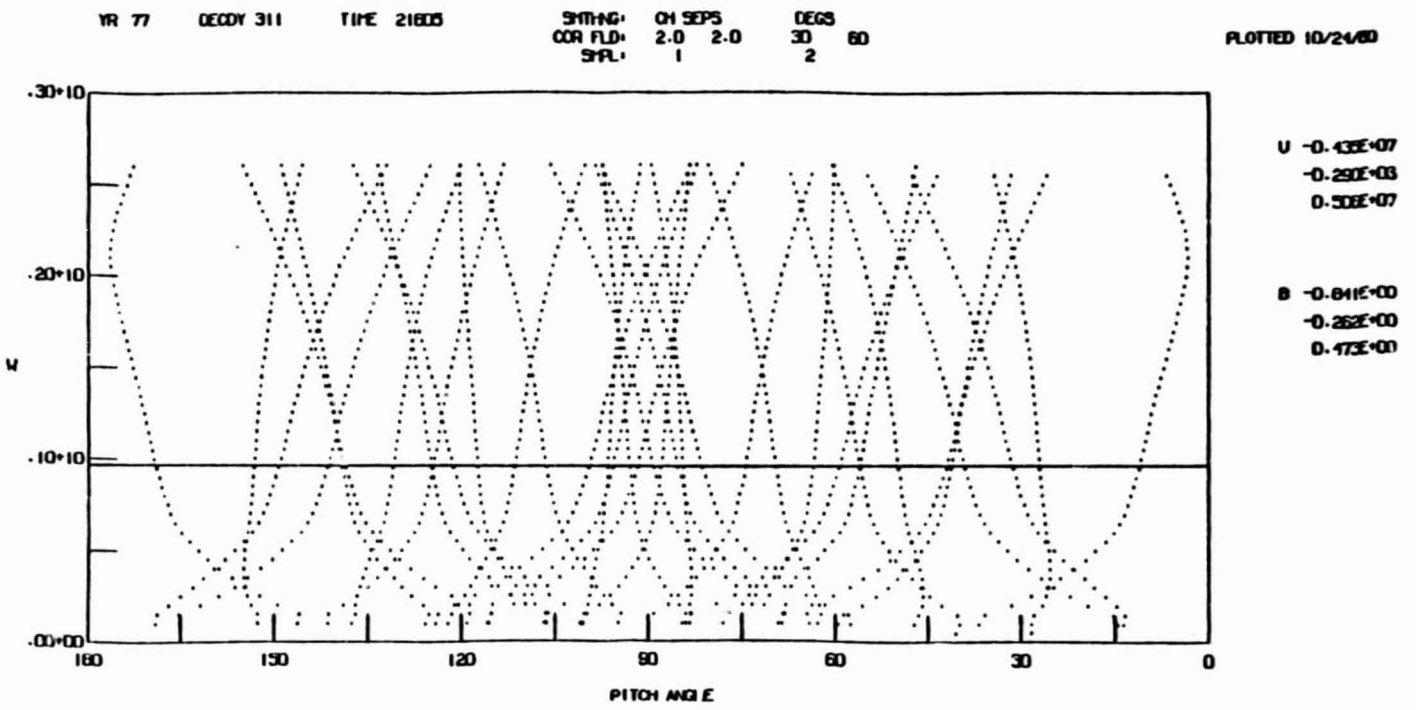
YR 77 DECDY 311 TIME 21605
SMTHNG: CH SEPS DEGS
COR FLD: 2.0 2.0 30 60
SMPL: 1 2
PLOTTED 10/24/80
.30+10
.20+10
.10+10
.00+00
W
180
150
120
90
60
30
0
PITCH ANGLE
U -0.435E+07
-0.290E+08
0.506E+07
B -0.841E+00
-0.262E+00
0.473E+00

Figure 6d

NASA

Technical Memorandum 83838

"Velocity- Space Synthesis of ISEE-1 Measurements of the Three-Dimensional Electron Distribution Function"

R. J. Fitzenreiter
J. D. Scudder

OCTOBER 1981

National Aeronautics and Space Administration

Goddard Space Flight Center
Greenbelt, Maryland 20771

PITCH ANGLE CROSS SECTION OF SMOOTHING FUNCTION

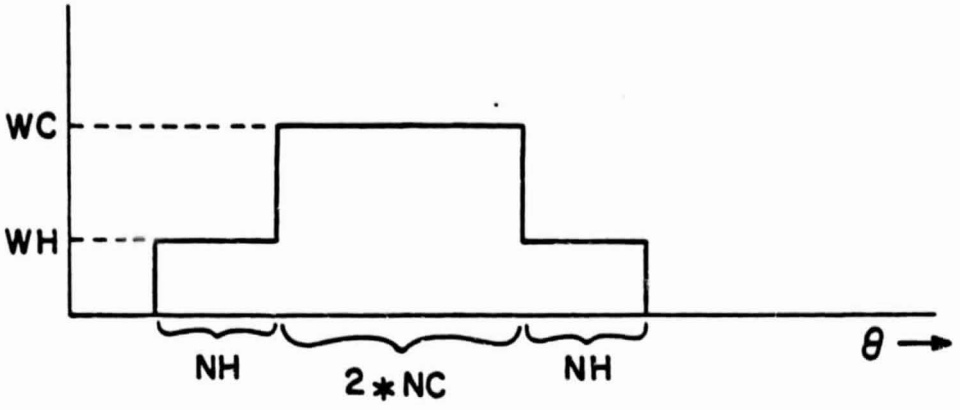

SPEED CROSS SECTION OF SMOOTHING FUNCTION

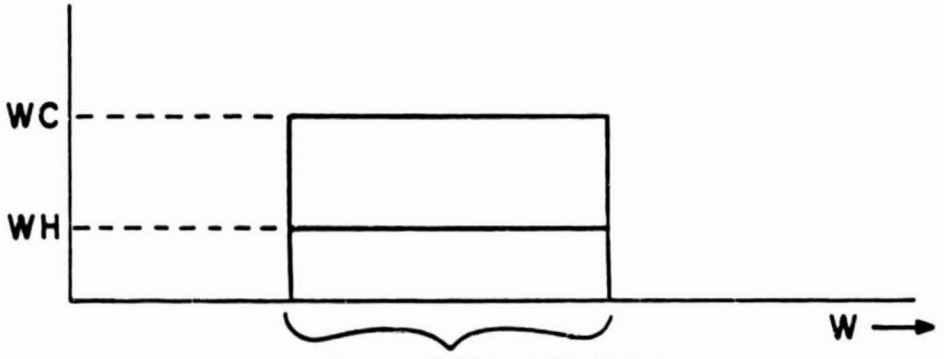

Figure 7